Electronic Supplementary Material (ESI) for Journal of Materials Chemistry A.

A symmetric direct ammonia fuel cell using ternary NiCuFe alloy embedded in carbon network as electrodes

Mengfei Zhang[a], Jie Zhang[b], Georgina Jeerh[a], Peimiao Zou[a], Boyao Sun[a], Marc Walker[c], Kui Xie[b], Shanwen Tao[a, d*]

[a] School of Engineering, University of Warwick, Coventry, CV4 7AL, UK

E-mail: s.tao.1@warwick.ac.uk

[b] Key Laboratory of Design and Assembly of Functional Nanostructures, Fujian Institute of Research on the Structure of Matter, Chinese Academy of Sciences, Fuzhou, Fujian 350002, China

[c] Department of Physics, University of Warwick, Coventry CV4 7AL, UK

[d] Department of Chemical Engineering, Monash University, Clayton, Victoria 3800, Australia

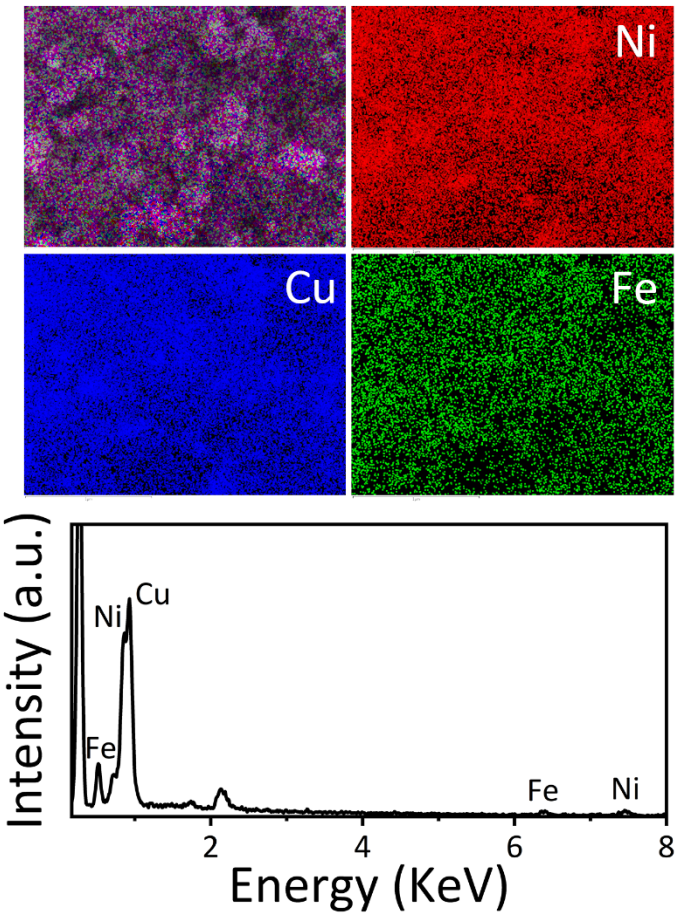

Figure S1. EDS mapping images and EDS spectrum of NiCuFe1/C.

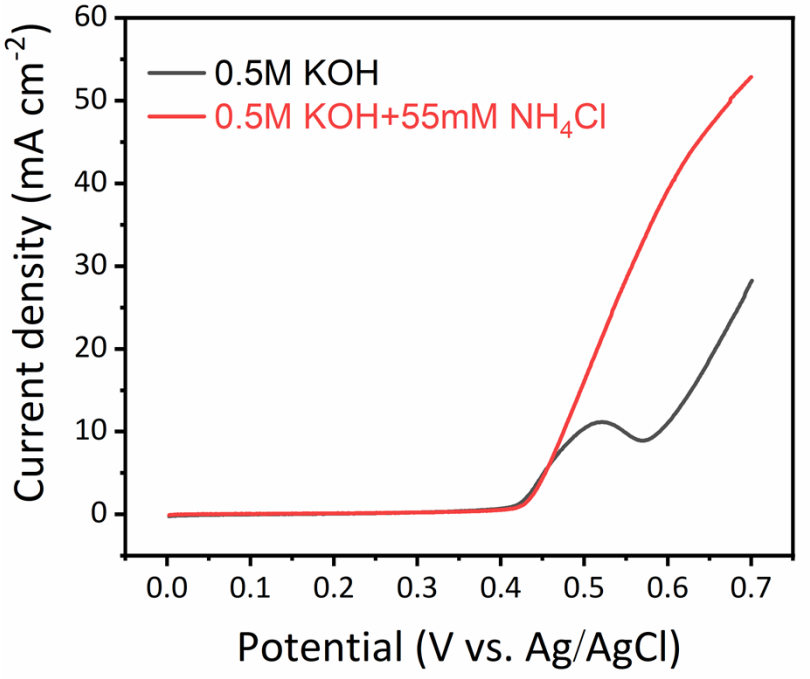

Figure S2. LSV curves of NiCuFe1/C in 0.5 M KOH, 0.5 M KOH+55 mM NH_4Cl at a scan rate of 2 mV s^{-1}.

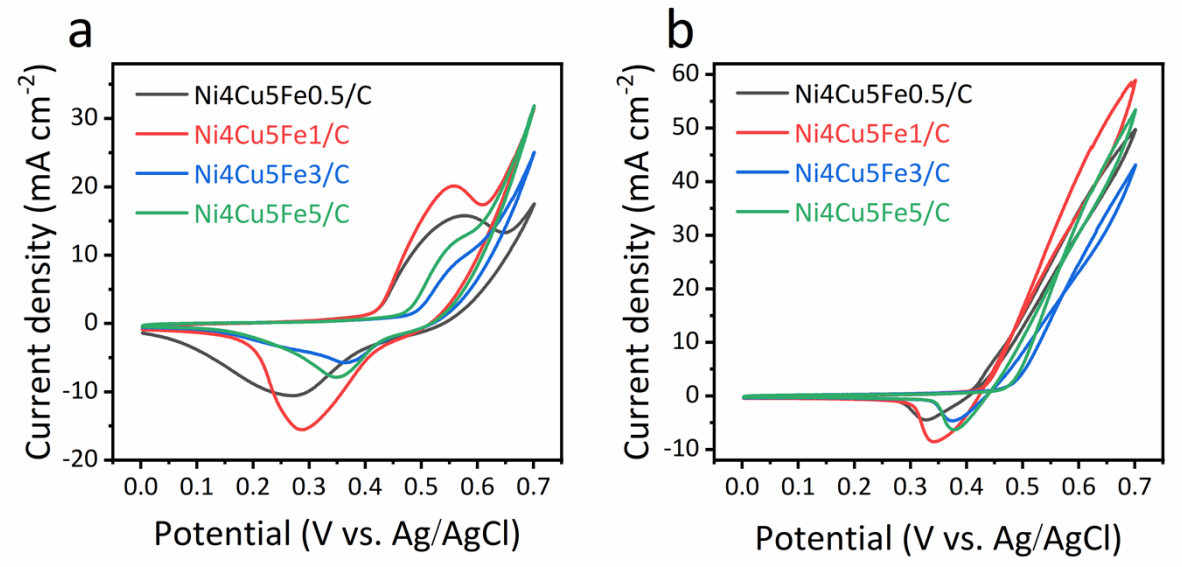

Figure S3. CV curves of NiCuFe0.5/C, NiCuFe1/C, NiCuFe3/C, NiCuFe5/C in (a) 0.5 M KOH, (b) 0.5 M KOH+55 mM NH_4Cl at a scan rate of 5 mV s^{-1}.

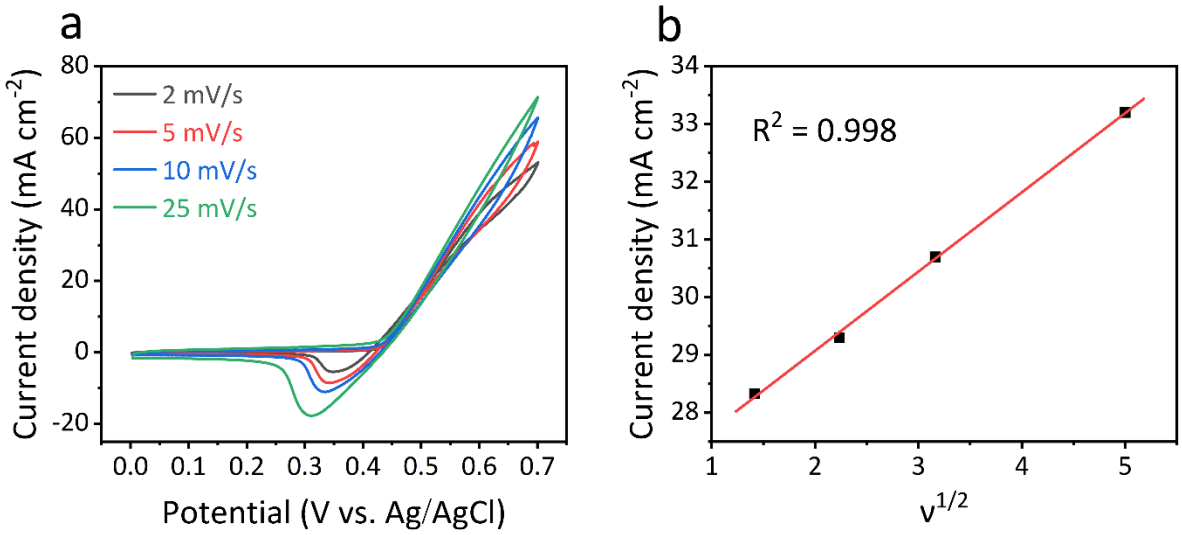

Figure S4. (a) CV curves of NiCuFe1/C in 0.5 M KOH+55 mM NH_4Cl at different scan rates. (b) plots of the square root of the current density vary with scan rate for NiCuFe1/C.

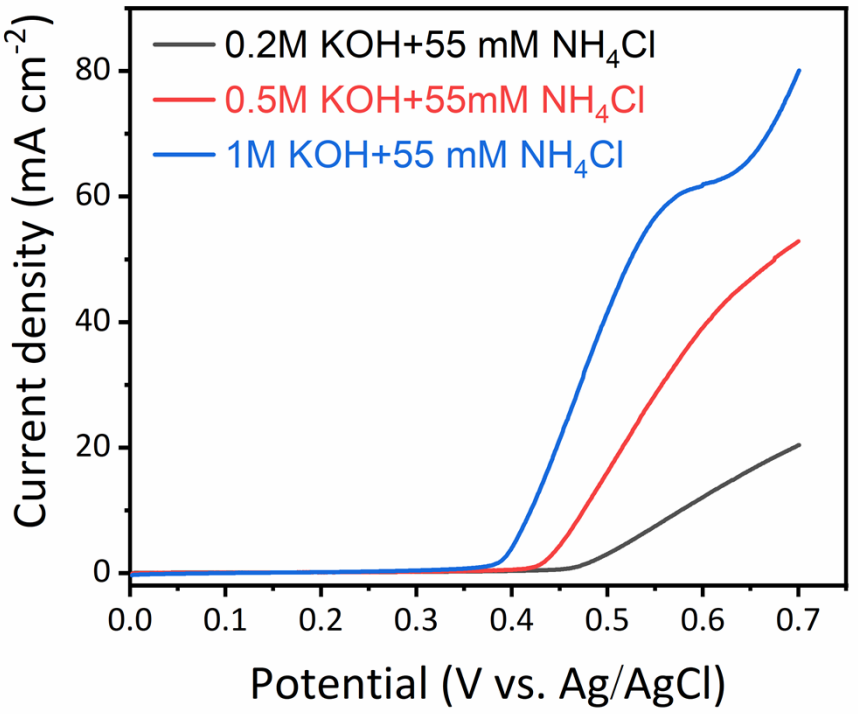

Figure S5. LSV curves of NiCuFe1/C in 55 mM NH_4Cl with different KOH concentration.

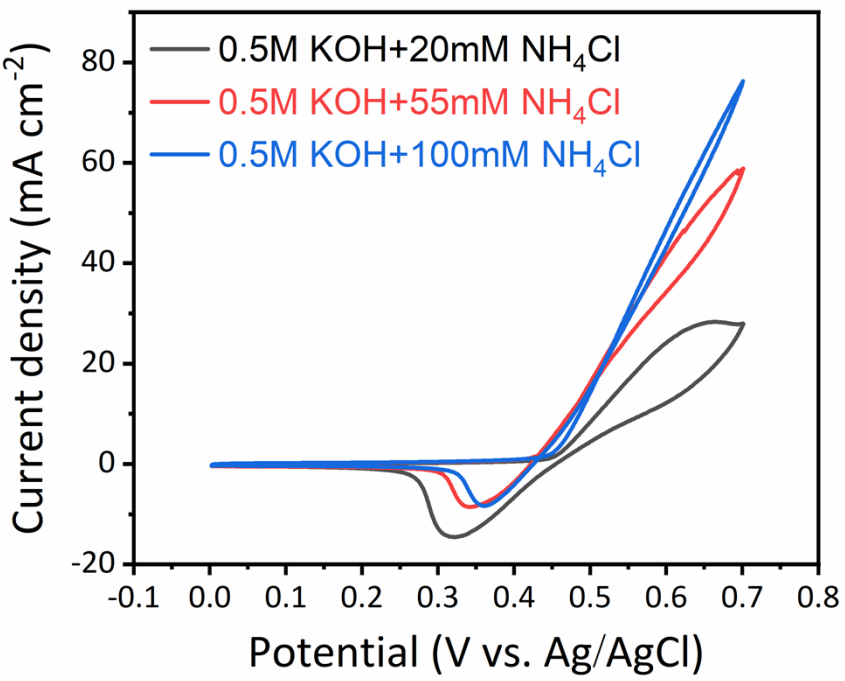

Figure S6. CV curves of NiCuFe1/C in 0.5 M KOH with different ammonia concentration at a scan rate of 5 mV s^{-1}.

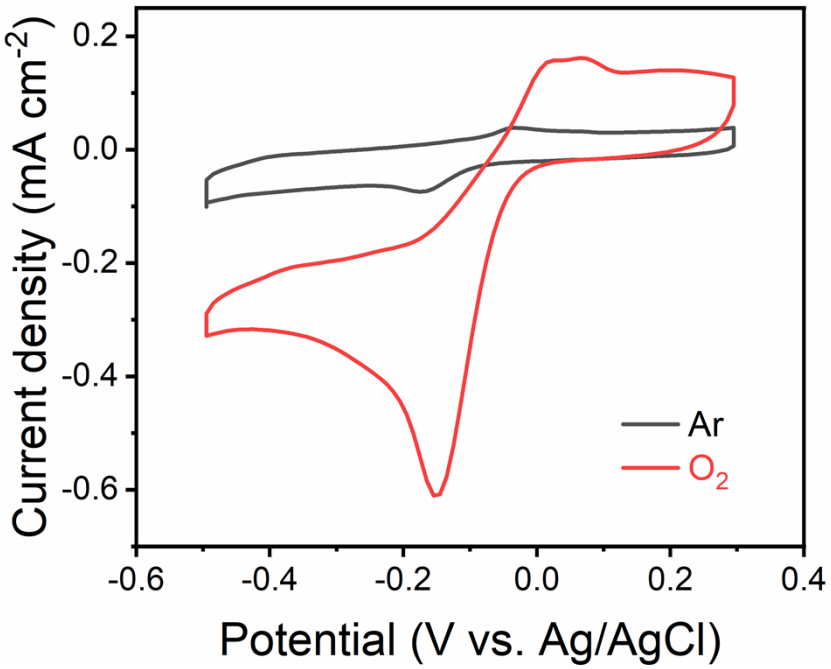

Figure S7. CV curves of NiCu/C in Ar or O_2-saturated 0.1 M KOH.

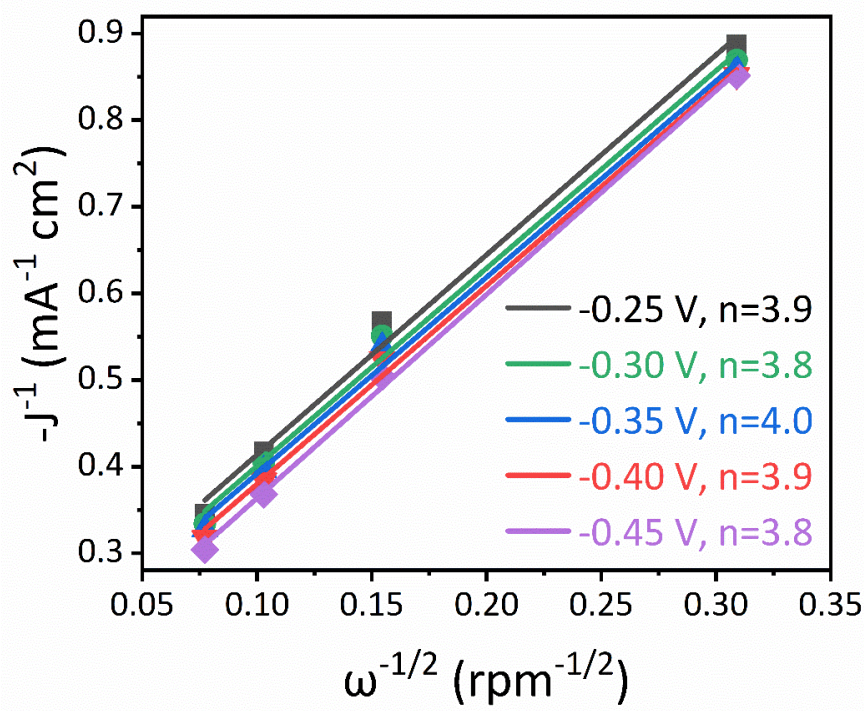

Figure S8. The fitted K-L plots of NiCuFe1/C at different potentials.

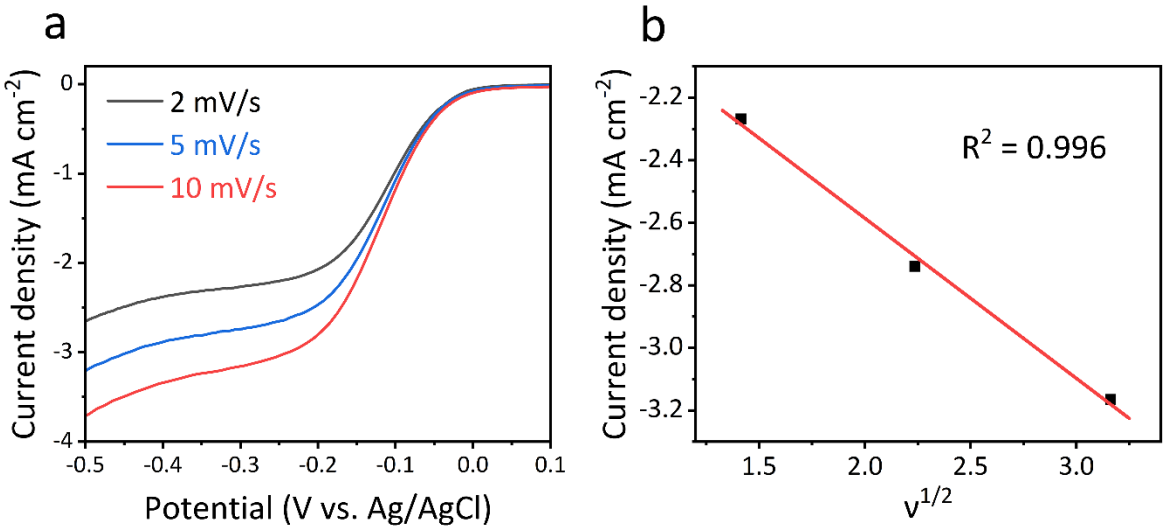

Figure S9. (a) LSV curves and (b) current density versus square root of the scan rate of NiCuFe1/C in O_2-saturated 0.1 M KOH at different scan rates.

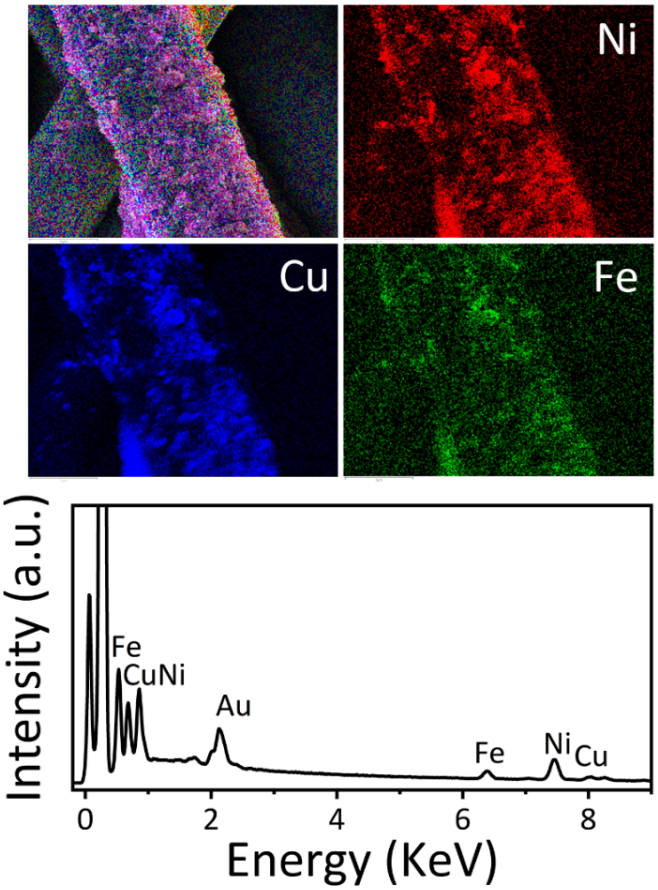

Figure S10. EDS Mapping images and EDS spectrum of NiCuFe1/C electrode before test.

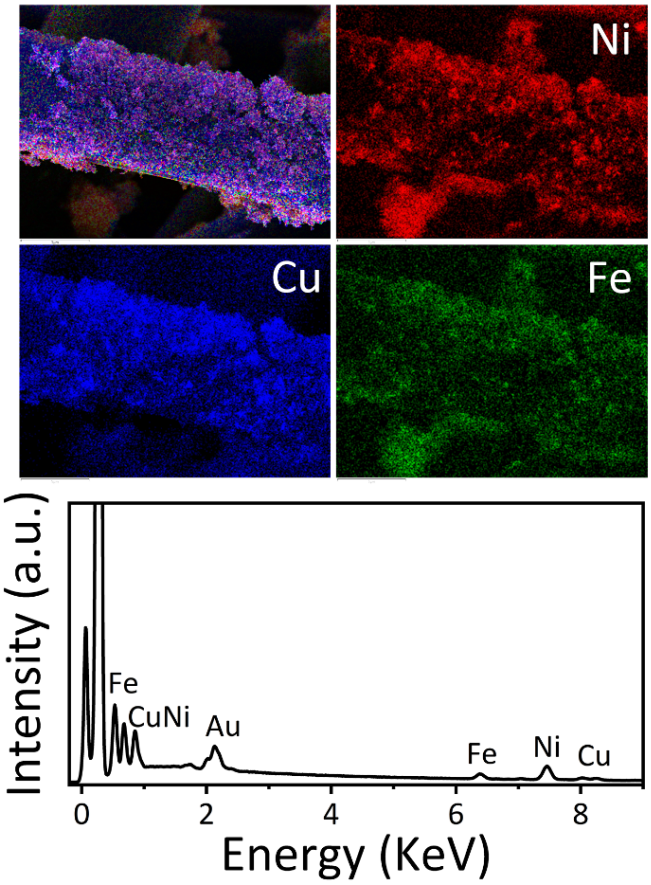

Figure S11. EDS Mapping images and EDS spectrum of NiCuFe1/C anode after test.

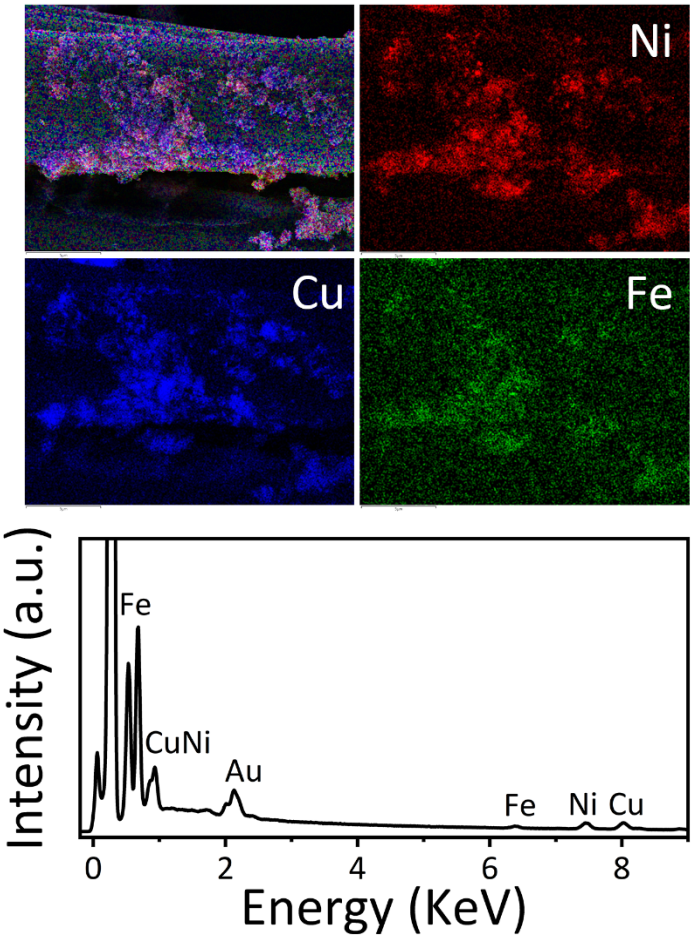

Figure S12. EDS Mapping images and EDS spectrum of NiCuFe1/C cathode after test.

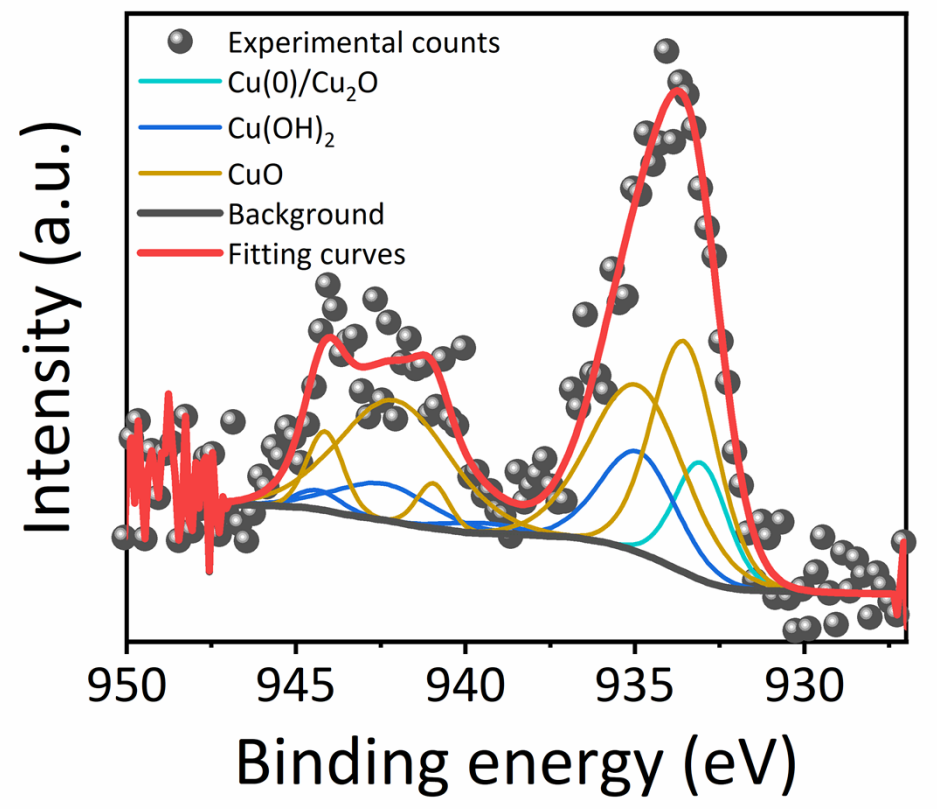

Figure S13. XPS spectrum of Cu2$p_{3/2}$ in Ni4Cu5Fe1/C anode.

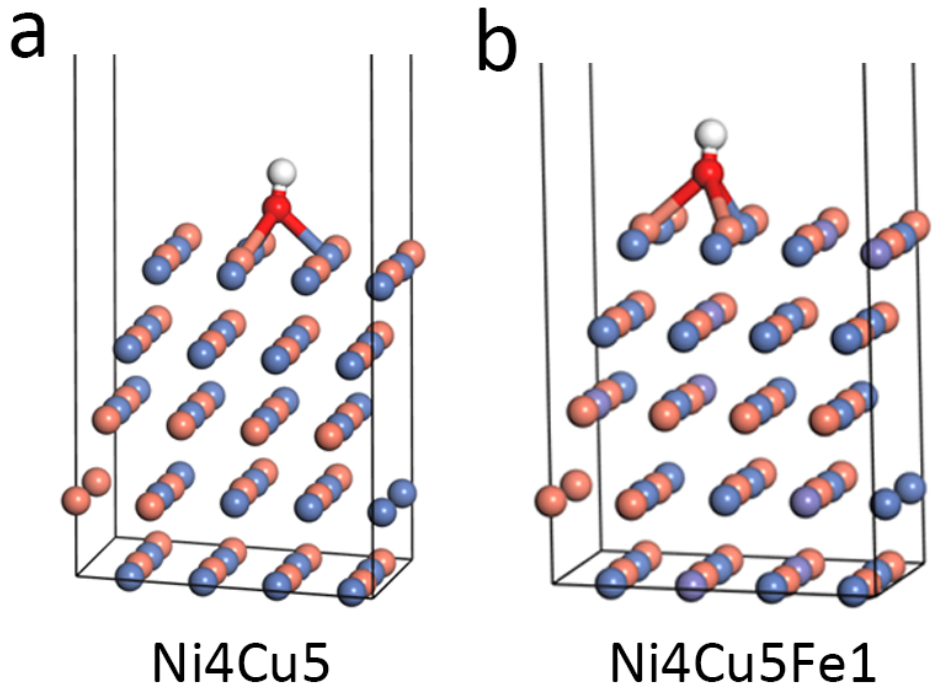

Figure S14. Slab model and OH adsorption on the surfaces of NiCu and NiCuFe1.

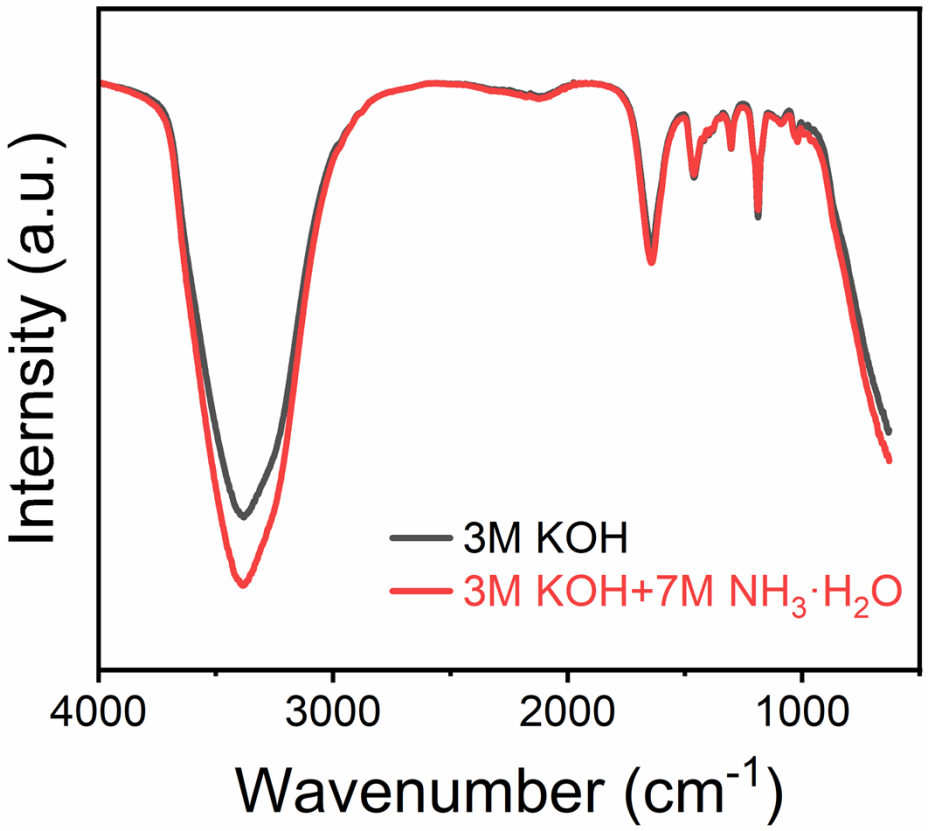

Figure S15. FTIR spectra of AEMs after immersed in 3 M KOH and 3 M KOH + 7 M $MH_3 \cdot H_2O$ for 24 h.

Table S1 The composition calculated from XRF results.

Samples	XRF results					The composition calculated from XRF
	Ni	Cu	Fe	P	S	
Ni4Cu5	41.1	57.4	0	0.64	0.42	Ni4Cu5.59
Ni4Cu5Fe0.5	39.8	52.9	2.83	0.64	0.40	Ni4Cu5.32Fe0.28
Ni4Cu5Fe1	37.8	53.2	7.71	0.58	0.37	Ni4Cu5.63Fe0.82
Ni4Cu5Fe3	33.2	45	20.5	0.53	0.34	Ni4Cu5.42Fe2.47

Table S2 Comparison of DAFC performance with literature results for DAFCs with non-precious metal catalysts in the electrodes.

Anode	Cathode	Fuel	T/°C	OCV/V	Peak current density/ mA cm^{-2}	Peak current density / mW cm^{-2}	Ref.
NiCu/C	$SrCo_{0.8}Cu_{0.1}Nb_{0.1}O_{3-\delta}$/C	1M NaOH + 35% $NH_3 \cdot H_2O$	25	0.45	~2.2	0.25	[1]
NiCu/C	$SrFe_{0.8}Cu_{0.1}Nb_{0.1}O_{3-\delta}$/C	1M NaOH + 5M $NH_3 \cdot H_2O$	25	0.46	~2.5	0.35	[2]
NiCu/C	α-MnO_2/C	3M $NH_3 \cdot H_2O$	25	0.39	2.1	0.35	[3]
Ni/C	MnO_2/C	35% $NH_3 \cdot H_2O$	25	0.77	~10	3.6	[4]
CDN/C	MnO_2/C	35% $NH_3 \cdot H_2O$	80	0.8	32	9	[5]
Ni4Cu5Fe1/C	Ni4Cu5Fe1/C	3M KOH+7M $NH_3 \cdot H_2O$	80	0.62	31	8.9	**This work**

References

1. P. Zou, S. Chen, R. Lan and S. Tao, *ChemSusChem*, 2019, **12**, 2788-2794.
2. P. Zou, S. Chen, R. Lan, J. Humphreys, G. Jeerh and S. Tao, *Int. J. Hydrog. Energy*, 2019, **44**, 26554-26564.
3. M. Zhang, P. Zou, G. Jeerh, S. Chen, J. Shields, H. Wang and S. Tao, *ACS Sustain. Chem. Eng.*, 2020, **8**, 12817-12824.
4. R. Lan and S. Tao, *ECS Electrochem. Lett.*, 2013, **2**, F37-F40.
5. R. Lan and S. Tao, *Electrochem. Solid-State Lett.*, 2010, **13**, B83-B86.